

Synthesis, Crystal Structure, and Photoluminescent Properties of Two Porous Pillared-Layer Metal-Organic Frameworks Constructed by Benzene-1,3,5-Tricarboxylic Acid and Bisimidazole Ligands

K. Wang*

School of Chemistry and Life Science, Anshan Normal University, Anshan, 114007 P.R. China

*e-mail: khwang16@163.com

Received March 14, 2018; revised November 23, 2018; accepted November 27, 2018

Abstract—Two pillared layer metal organic frameworks, namely $\{[\text{Co}_3(\text{Btc})_2(\text{Bib})_3(\text{H}_2\text{O})_2] \cdot 7\text{H}_2\text{O}\}_n$ (**I**) and $\{[\text{Cd}_2(\text{Btc})(\text{Bib})_2(\text{Fma})(\text{H}_2\text{O})] \cdot \text{H}_2\text{O}\}_n$ (**II**), where H_3Btc is benzene-1,3,5-tricarboxylic acid, Fma is formate anion and Bib is 1,4-bis(1-imidazolyl)benzene, have been successfully synthesized by solvothermal method and structurally characterized by element analysis, IR spectroscopy, as well as single crystal X-ray diffraction and power X-ray diffraction (CIF files CCDC nos. 1829267 (**I**), 1829266 (**II**)). In the complexes **I** and **II**, the full deprotonated aromatic polycarboxylate take the same coordination mode to bridging four metal ions but result in different 2D network, which are further pillared by bib ligands to form 3D architectures with point symbol of $(4^2.6^4)_2(4^2.6^7.8)_2(6^4.8^2)$ and $(4^2.6^3.8)(4^2.6^4)(4^2.6^7.8)$, respectively. The photoluminescent property of complex **II** is also reported.

Keywords: pillared-layer MOFs, bisimidazole ligands, benzene-1,3,5-tricarboxylic acid, crystal structure

DOI: 10.1134/S1070328419040092

INTRODUCTION

Metal organic frameworks (MOFs) are new porous materials that constructed by metal ions or metal clusters and organic ligands through coordination bonds in themselves-assembly process, and exhibit unique and excellent properties, such as selective adsorption, fluorescent sensing, catalysis, drug delivery and so on [1–4]. However, it is difficult but desirable work for chemist to synthesize MOFs with prospective architectures, due to not only coordination preference of metal ions, coordination capacity and geometrical characters of ligands but also other intricate factors, such as temperature, solvents, counter anions and pH values influencing its final architectures in themselves-assembly process [5–10]. Recently, it has been proved to be an effective and controllable synthetic strategy for pillared-layer motifs to obtain porous MOFs with desired structure and properties, and sizes and hydrophobicity/hydrophilicity of their cavities may be adjusted through different pillar ligands and postsynthetic modification [11–17]. Porous pillared-layer MOFs based rigid bisimidazole ligands such as 1,4-bis(imidazolyl)benzene (Bib) were less reported in

comparison with a large number of interpenetrating MOFs constructed by bisimidazole ligands [18–26]. We have reported three pillared-layer MOFs in which 2D networks constructed by imidazole-4,5-dicarboxylate and metal ions were pillared by Bib or 4,4-bis(1-imidazolyl)biphenyl ligands lately [27]. Benzene-1,3,5-tricarboxylic acid (H_3Btc) with symmetrical structure was an appropriate ligand to construct different 2D networks, which may be further connected by pillar ligands to generate pillared-layer MOFs [28–30]. Based on the above considerations, we used H_3Btc and Bib as ligands to react with $\text{Co}(\text{II})$ or $\text{Cd}(\text{II})$ salts under solvothermal condition and successfully obtained two pillared-layer MOFs, $\{[\text{Co}_3(\text{Btc})_2(\text{Bib})_3(\text{H}_2\text{O})_2] \cdot 7\text{H}_2\text{O}\}_n$ (**I**) and $\{[\text{Cd}_2(\text{Btc})(\text{Bib})_2(\text{Fma})(\text{H}_2\text{O})] \cdot \text{H}_2\text{O}\}_n$ (**II**), where Fma is formate anion. Complexes **I** and **II** were characterized by IR, elemental analysis, powder X-ray diffraction (PXRD) and single crystal X-ray diffraction, their photoluminescence properties were also studied.

EXPERIMENTAL

Materials and methods. All commercially available chemicals and solvents are of reagent grade and were used as received without further purification. Elemental analyses were performed on a Perkin-Elmer 240C Elemental Analyzer. FT-IR spectra were recorded on Nicolet IR-470 instrument using KBr pellets. PXRD data were collected on a Bruker D8 Advance X-ray diffractometer with CuK_α radiation ($\lambda = 1.5418 \text{ \AA}$). The photoluminescence properties of compound **II** in solid state was measured on a Perkin-Elmer LS55 spectrophotometer at room temperature.

Synthesis of I. A mixture of $\text{CoCl}_2 \cdot 6\text{H}_2\text{O}$ (0.1 mmol, 0.0237 g), H_3Btc (0.1 mmol, 0.0210 g), Bib (0.1 mmol, 0.0210 g), NaOH (0.3 mmol, 0.012 g), H_2O (10 mL) and DMF (2 mL) was stirred for 1 h in air, then was transferred to and sealed in a 25 mL Teflon-lined reactor, and heated in an oven to 110°C for 72 h. After cooling to room temperature, brown block crystals of **I** were collected by filtration and washed with water and DMF several times.

For $\text{C}_{54}\text{H}_{54}\text{N}_{12}\text{O}_{21}\text{Co}_3$

Anal. calcd., %	C, 46.87	N, 12.15	H, 3.93
Found, %	C, 46.81	N, 12.09	H, 3.96

IR (KBr pellet; ν , cm^{-1}): 3396 s, 2362 s, 1613 s, 1527 s, 1427 s, 1361 s, 1062 s, 837 s, 764 s, 711 s, 658 s.

Synthesis of II was carried out by the similar solvothermal procedure as that for synthesis of **I** except that CdSO_4 (0.1 mmol, 0.0208 g) instead of $\text{CoCl}_2 \cdot 6\text{H}_2\text{O}$. After cooling to room temperature, colorless block crystals of **II** were collected by filtration and washed with water and DMF several times.

For $\text{C}_{34}\text{H}_{28}\text{N}_8\text{O}_{10}\text{Cd}_2$

Anal. calcd., %	C, 43.75	N, 12.01	H, 3.02
Found, %	C, 43.36	N, 12.08	H, 2.97

IR (KBr pellet; ν , cm^{-1}): 3436 s, 3111 s, 2819 s, 2355 s, 1619 s, 1527 s, 1314 s, 1261 s, 1129 s, 1069 s, 956 s, 837 s, 758 s, 645 s, 519 s.

X-ray crystallography. Crystallographic diffraction data for complexes **I** and **II** were recorded on SMART CCD 1000 X-ray single-crystal diffratometer with MoK_α radiation ($\lambda = 0.71073 \text{ \AA}$) at room temperature. All the structures were solved by ShelXT structure solution program and refined with ShelXL refinement package within OLEX 1.2 [31, 32]. The phase purity of

bulk crystal samples was confirmed by PXRD. The crystallographic data and structure refinement parameters for the two compounds are given in Table 1, and selected bond lengths and angles are listed in Table 2.

Supplementary material has been deposited with the Cambridge Crystallographic Data Centre (CCDC nos. 1829267 (**I**), 1829266 (**II**); deposit@ccdc.cam.ac.uk or <http://www.ccdc.cam.ac.uk>).

RESULTS AND DISCUSSION

The results of single crystal X-ray diffraction reveals the complex **I** is a pillared-layer 3D framework. As shown in Fig. 1a, there are two independent cobalt atoms: Co(1) is hexa-coordinated with two oxygen atoms of two Btc ligands, two nitrogen atoms of two Bib ligands and two water molecules to complete a distorted octahedral sphere with N_2O_4 donor set, and Co(2) also exhibited a distorted octahedral geometry with N_2O_4 donor set but completed by four oxygen atoms from three different Btc ligands and two nitrogen atoms from two Bib ligands. The Co–O bond distances rang from 2.040(4) to 2.257(4) \AA and Co–N bond distances rang from 2.120(5) to 2.142(5) \AA which can be compared with reported values [33]. The completely deprotonated Btc ligands acts as μ_4 -connector to link four Co ions with bidentate chelating, $\mu_2\text{-}\eta_1\text{:}\eta_1$ bridging and monodentate coordination modes, generating a 2D Co-Btc network as shown in Fig. 1b. In the network, the two Btc ligands connect $[\text{Co}_2(\text{COO})_4]$ units with Co–Co distance of 4.307 \AA to form a 1D ladder chains. These chains are further connected by $[\text{Co}(\text{COO})_2]$ unit to form an extended 2D layer structure. The 2D Co-Btc layer are further pillared by Bib ligands via Co–N connections to generate a 3D pillar-layered structure (Fig. 1c). PLATON analysis suggested that the porous of **I** consists of voids of 307.6 \AA^3 that represent 20.1% of unit cell volume of **I** (1534.0 \AA^3) [34]. Topology analyses display that the pillared-layer 3D framework of complex **I** can be simplified as a 4,5-connected topological LEDPIU structure with point symbol of $(4^2\cdot 6^4)_2(4^2\cdot 6^7\cdot 8)_2(6^4\cdot 8^2)$ (Fig. 1d), in which Btc and Co^{2+} ions act as 4-connected nodes and Co(1) ions are regarded as 5-connected nodes, Bib ligands as linkers [35].

When CdSO_4 instead of CoCl_2 in synthesis of compound **I** resulted, a new 3D pillared-layer metal-

Table 1. Crystallographic data and structure refinement parameters for complex **I** and **II**

Parameter	Value	
	I	II
Formula weight	1383.88	933.46
Crystal system	Triclinic	Triclinic
Space group	$P\bar{1}$	$P\bar{1}$
a , Å	10.052(15)	10.241(7)
b , Å	12.567(19)	13.138(9)
c Å	13.46(2)	14.032(10)
α , deg	85.375(19)	88.563(12)
β , deg	70.604(16)	78.638(13)
γ , deg	73.110(17)	72.049(10)
V	1534(4)	1760(2)
Z	1	2
ρ_{calcd} , g cm ⁻³	1.498	1.762
μ , mm ⁻¹	0.887	1.279
$F(000)$	711.0	928
θ Range, deg	3.208–50.016	1.481–28.358
Reflections collected	8758	11176
Independent reflections (R_{int})	5316 (0.0342)	8169 (0.0306)
Reflections with $I > 2\sigma(I)$	3697	5284
Number of parameters	431	490
R_1 ($I > 2\sigma(I)$)*	0.0514	0.0499
wR_2 *	0.1519	0.1223
GOOF	1.027	1.027
Largest diff. peak and hole, e Å ⁻³	0.41 and -0.39	0.876 and -0.928

* $R = \sum ||F_{\text{o}}| - |F_{\text{c}}|| / \sum |F_{\text{o}}|$, $R_w = [\sum [w(F_{\text{o}}^2 - F_{\text{c}}^2)^2] / \sum w(F_{\text{o}}^2)^2]^{1/2}$.

Table 2. Selected bond distances (Å) and angles (deg)*

Bond	<i>d</i> , Å	Bond	<i>d</i> , Å
I			
Co(1)–N(5)	2.138(5)	Co(2)–O(5) ^{#3}	2.257(4)
Co(1)–O(4)	2.099(4)	Co(2)–N(3)	2.120(5)
Co(1)–O(7)	2.116(4)	Co(2)–O(2)	2.068(4)
Co(2)–N(1)	2.142(5)	Co(2)–O(6) ^{#3}	2.186(4)
Co(2)–O(1) ^{#2}	2.040(4)		
II			
Cd(1)–O(1)	2.401(4)	Cd(1)–O(1) ^{#1}	2.383(4)
Cd(1)–O(3)	2.276(4)	Cd(1)–O(9)	2.360(5)
Cd(1)–N(5)	2.308(4)	Cd(1)–N(8) ^{#2}	2.288(5)
Cd(2)–O(5) ^{#3}	2.395(4)	Cd(2)–O(6) ^{#3}	2.397(4)
Cd(2)–O(7)	2.275(4)	Cd(2)–O(8) ^{#4}	2.307(4)
Cd(2)–N(1)	2.269(4)	Cd(2)–N(4) ^{#2}	2.293(5)
O(1)–Cd(1) ^{#1}	2.383(4)		
Angle	ω , deg	Angle	ω , deg
I			
O(4)Co(1)N(5) ^{#1}	83.24(18)	O(4)Co(1)N(5)	96.77(18)
O(4)Co(1)O(7) ^{#1}	92.12(14)	O(4)Co(1)O(7)	87.88(14)
O(7)Co(1)N(5)	87.07(16)	O(7)Co(1)N(5) ^{#1}	92.93(16)
N(1)Co(2)O(5) ^{#2}	95.50(16)	N(1)Co(2)O(6) ^{#2}	85.15(14)
N(3)Co(2)O(5) ^{#2}	88.09(16)	N(3)Co(2)O(6) ^{#2}	96.07(15)
O(1) ^{#3} Co(2)O(6) ^{#2}	97.83(12)	O(2)Co(2)N(1)	93.46(14)
O(2)Co(2)N(3)	87.30(15)	O(2)Co(2)O(5) ^{#2}	89.64(14)
II			
O(1) ^{#1} Cd(1)O(1)	72.20(16)	O(3)Cd(1)O(1)	85.05(14)
O(3)Cd(1)N(5)	83.13(16)	O(3)Cd(1)N(8) ^{#2}	95.05(16)
O(9)Cd(1)O(1) ^{#1}	90.06(19)	N(5)Cd(1)O(1)	90.57(15)
N(5)Cd(1)O(1) ^{#1}	86.92(16)	N(5)Cd(1)O(9)	85.63(17)
N(8) ^{#2} Cd(1)O(9)	92.94(17)	O(7)Cd(2)O(5) ^{#3}	86.73(13)
O(7)Cd(2)N(4) ^{#2}	86.87(15)	N(1)Cd(2)O(5) ^{#3}	92.80(15)
N(1)Cd(2)O(6) ^{#3}	87.95(14)	N(1)Cd(2)O(8) ^{#4}	92.04(15)
N(1)Cd(2)C(6) ^{#3}	90.36(15)	N(4) ^{#2} Cd(2)O(5) ^{#3}	91.55(16)
N(4) ^{#2} Cd(2)O(6) ^{#3}	89.05(15)	N(4) ^{#2} Cd(2)O(8) ^{#4}	81.36(15)

* Symmetry codes: ^{#1} 1–*x*, −*y*, −*z*; ^{#2} −1+*x*, *y*, *z*; ^{#3} −*x*, 1−*y*, 1−*z* (**I**); ^{#1} −*x*, −*y*+1, −*z*+1; ^{#2} *x*+1, *y*−1, *z*; ^{#3} *x*−1, *y*, *z*; ^{#4} −*x*, −*y*+2, −*z* (**II**).

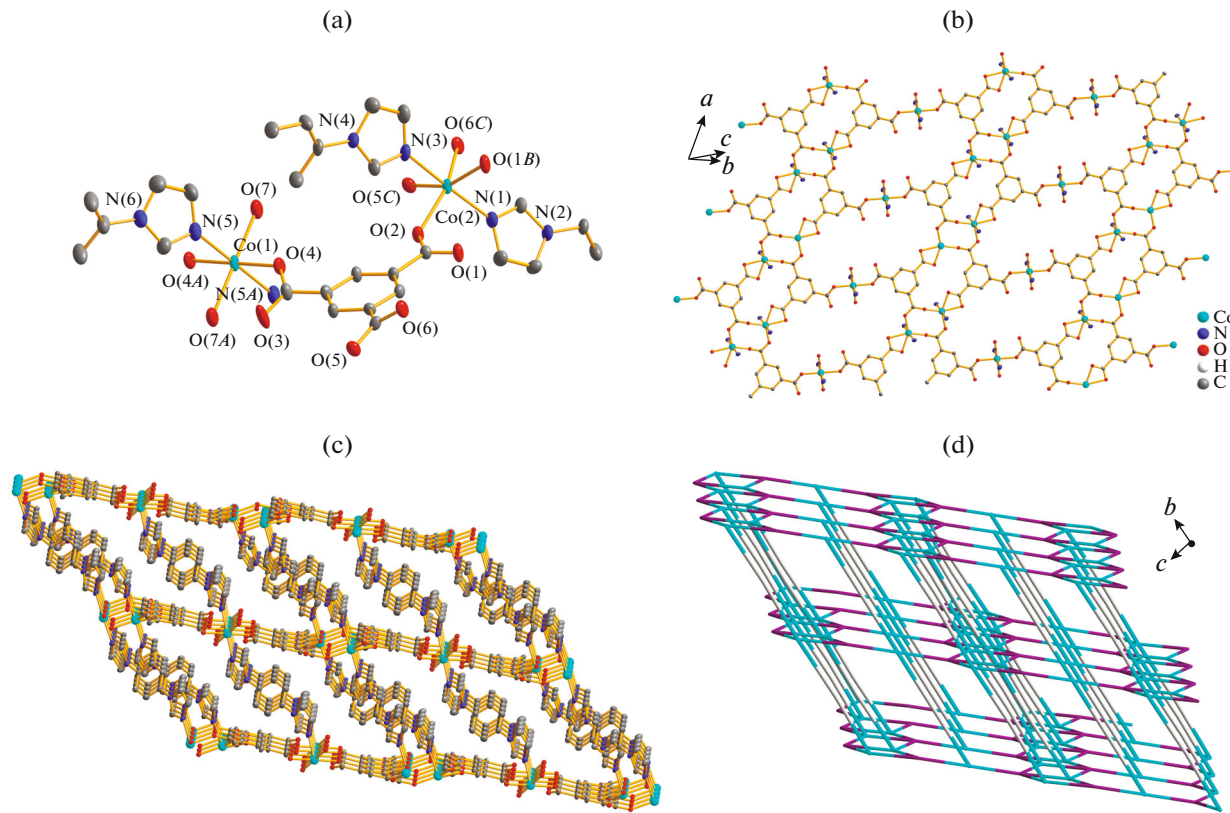


Fig. 1. The coordination environment of Co^{2+} ions in compound I (a); the 2D network constructed by Btc and Co^{2+} ions (b); the 3D pillared-layer structure of compound I (c); the topology of the $(4,5)$ -connected network with point symbol of $(4^2.6^4)_2(4^2.6^7.8)_2(6^4.8^2)$ in compound I (d).

organic framework. As shown in Fig. 2a, $\text{Cd}(1)$ displays a distorted octahedral sphere, provided by one Btc ligand via a carboxyl oxygen atom, two oxygen atom from two formate anion, one water molecule and two Bib ligands via imidazolyl nitrogen. The formate acid is the hydrolysis product of DMF under solvothermal condition [36]. $\text{Cd}(2)$ is octahedral coordinated by four oxygen atoms from three Btc ligands and two nitrogen atoms from two Bib ligands. The $\text{Cd}–\text{O}$ bond distance fall in the range of 2.275(4)–2.401(4) Å, and the $\text{Cd}–\text{N}$ bond distance vary from 2.269(4) to 2.308(4) Å. In the complex **II**, the ligand of Btc adopts the same coordination mode as in complex I, linking the Cd^{2+} ions to form 1D ladder chains but the adjacent chains are connected by $[\text{Cd}_2(\text{Fma})_2]$ cluster, resulting a different 2D network (Fig. 2b). The 2D network are linked by Bib pillars to form a 3D porous framework (Fig. 2c). Based on chemical topological view, the $\text{Cd}(2)$ ions can be abstracted as five connected

nodes, and $\text{Cd}(1)$ ions and Btc ligands as four connected nodes, while Bib ligands and Fma anions acts as linner linker. Thus the overall 3D network of **II** can be rationalized as a bimodal 4,5-connected new network with point symbol of $(4^2.6^3.8)(4^2.6^4)(4^2.6^7.8)$.

The photoluminescent properties of complex **II** and free ligands have been investigated in solid state at room temperature. As shown in Fig. 3, the main emission peak of free Bib and H_3Btc ligands are 387 nm ($\lambda_{\text{ex}} = 332$ nm) and 400 nm ($\lambda_{\text{ex}} = 352$ nm), which is probably attributed to $\pi^* \rightarrow \pi$ or $\pi^* \rightarrow n$ transitions, and complex **II** exhibits luminescent emission peaks at 454 nm ($\lambda_{\text{ex}} = 391$ nm), which is red shifted about 67 nm in comparison with free ligands of Bib . The emission of complex **II** is neither metal-to-ligand charge transfer nor ligand-to-metal charge transfer in nature, and may be assigned to intraligand fluorescence emission of Bib ligands [37, 38].

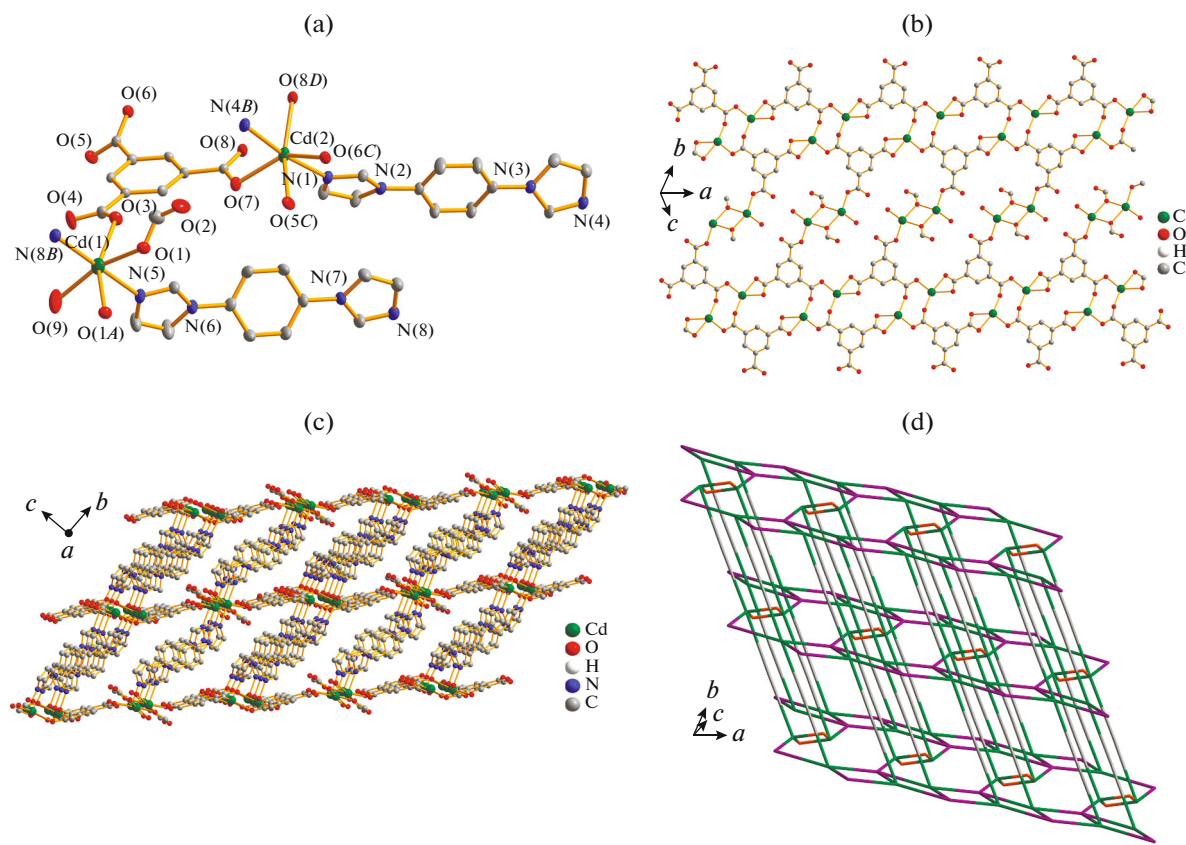


Fig. 2. The coordination environment of Cd²⁺ ions in compound **II** (a); the 2D network constructed by Btc and Cd²⁺ ions (b); the 3D pillared-layer structure of compound **II** (c); the topology of the (4,5)-connected network with point symbol of (4².6³.8)(4².6⁴)(4².6⁷.8) in compound **II** (d).

FUNDING

This work was supported by the Foundation of Anshan Science and Technology Program (no. 2014MS15) and Natural Science Foundation of Liaoning Province (no. 20180550712).

REFERENCES

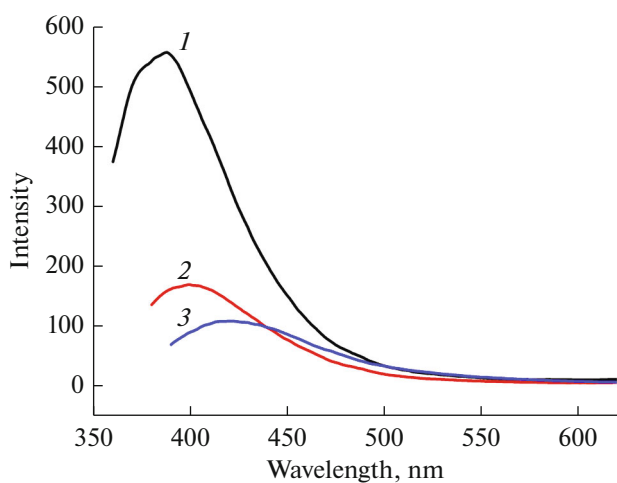


Fig. 3. The solid-state luminescent spectra of free ligands: Bib (1), H₃Btc (2) and compound **II** (3).

1. Li, J.R., Ma, Y., McCarthy, M.C., et al., *Coord. Chem. Rev.*, 2011, vol. 255, p. 1791.
2. Sun, C.-Y., Qin, C., Wang, C.-G., et al., *Adv. Mater.*, 2011, vol. 23, p. 5629.
3. Singha, D.K. and Mahata, P., *Inorg. Chem.*, 2015, vol. 54, p. 6373.
4. Katz, M.J., Moon, S.Y., Mondloch, J.E., et al., *Chem. Sci.*, 2015, vol. 6, p. 2286.
5. Chen, L., Zhang, L., Li, S.-L., et al., *CrystEngComm*, 2013, vol. 15, p. 8214.
6. Li, Z.-X., Chu, X., Cui, G.-H., et al., *CrystEngComm*, 2011, vol. 13, p. 1984.
7. Wei, G.-H., Yang, J., Ma, J.-F., et al., *Dalton Trans.*, 2008, p. 3080.

8. Ma, J., Jiang, F., Chen, L., et al., *CrystEngComm*, 2012, vol. 14, p. 4181.
9. Dey, S.K., Mitra, P., and Mukherjee, A., *Cryst. Growth Des.*, 2015, vol. 15, p. 706.
10. Liang, G., Liu, Y., Zhang, X., et al., *CrystEngComm*, 2014, vol. 16, p. 9896.
11. Yin, Z., Zhou, Y.-L., Zeng, M.-H., et al., *Dalton Trans.*, 2015, vol. 44, p. 5258.
12. Chang, Z., Zhang, D.-S., Chen, Q., et al., *Inorg. Chem.*, 2011, vol. 50, p. 7555.
13. Hernández-Ahuactz, I.F., Höpfl, H., Barb, V., et al., *Eur. J. Inorg. Chem.*, 2008, vol. 2008, p. 2746.
14. Yang, Q., Ren, S.-S., Hao, Y., et al., *Inorg. Chem.*, 2016, vol. 55, p. 4951.
15. Schwedler, I., Henke, S., Wharmby, M.T., et al., *Dalton Trans.*, 2016, vol. 45, p. 4230.
16. Jeong, S., Kim, D., Song, X., et al., *Chem. Mater.*, 2013, vol. 25, p. 1047.
17. Lin, Z.-J., Liu, T.-F., Xu, B., et al., *CrystEngComm*, 2011, vol. 13, p. 3321.
18. Wang, K.-H. and Gao, E.-J., *J. Coord. Chem.*, 2014, vol. 67, p. 563.
19. Yang, G.-S., Lan, Y.-Q., and Zhang, H.-Y., *CrystEngComm*, 2009, vol. 11, p. 247.
20. Yang, W., Guo, M., Yi, F.-Y., et al., *Cryst. Growth Des.*, 2012, vol. 12, p. 5529.
21. Yang, Q., Chen, X., Cui, J., et al., *Cryst. Growth Des.*, 2012, vol. 12, p. 4072.
22. Wang, F., Ke, X., and Zhao, J., *Dalton Trans.*, 2011, vol. 40, p. 11856.
23. Zhang, L., Yao, Y.-L., Che, Y.-X., et al., *Cryst. Growth Des.*, 2010, vol. 10, p. 528.
24. Xu, J., Zhang, M.-D., and Chen, M.-D., *Polyhedron*, 2015, vol. 90, p. 28.
25. Guo, F., Zhu, B., and Xu, G., *J. Solid State Chem.*, 2013, vol. 199, p. 42.
26. Zhang, C., Hao, H., Shi, Z., et al., *CrystEngComm*, 2014, vol. 16, p. 5662.
27. Wang, K.H., *J. Coord. Chem.*, 2017, vol. 70, p. 3982.
28. Liu, Y., Li, N., Li, L., et al., *CrystEngComm*, 2012, vol. 14, p. 2080.
29. Lee, C.H., Wu, J.Y., Lee, G.H., et al., *Cryst. Growth Des.*, 2014, vol. 14, p. 5608.
30. Mu, Y., Fu, J., and Song, Y., *Cryst. Growth Des.*, 2011, vol. 11, p. 2183.
31. Dolomanov, O.V., Bourhis, L.J., Gildea, R.J., et al., *J. Appl. Cryst.*, 2009, vol. 42, p. 339.
32. Sheldrick, G.M., *Acta Crystallogr., Sect. C: Struct. Chem.*, 2015, vol. 71, p. 3.
33. Sun, L.-X., Qi, Y., Che, Y.-X., et al., *Cryst. Growth Des.*, 2009, vol. 9, p. 2995.
34. Spek, A.L., *J. Appl. Cryst.*, 2003, vol. 36, p. 7.
35. Pan, J., Jiang, F.-L., Yuan, D.-Q., et al., *CrystEngComm*, 2013, vol. 15, p. 5673.
36. Wang, Z., Wang, K.H., Zhao, L.J., et al., *Koord. Khim.*, 2016, vol. 42, no. 12, p. 751. doi 10.7868/S0132344X16120082
37. Chen, S.-S., Fan, J., and Okamura, T., *Cryst. Growth Des.*, 2010, vol. 10, p. 812.
38. Yang, Y.-Q., Su, C.-F., and Zhang, J.-D., *J. Coord. Chem.*, 2016, vol. 69, p. 3762.